Desalination and Water Treatment
www.deswater.com

doi: 10.5004/dwt.2023.29457

291 (2023) 72–91
April

Model development for the treatment of industrial wastewaters by the coagulation–flocculation process: an easy tool for linking experimental to theoretical data

Slimane El Harfaoui[a], Zakia Zmirli[b], Ali Mohssine[a], Anas Driouich[a], Brahim Sallek[b], Khalid Digua[a], Hassan Chaair[a,*]

[a]*Laboratory of Process Engineering and Environment, Faculty of Sciences and Technology, University Hassan II, BP 146 Mohammedia 28 806, Morocco, emails: slimane.elharfaoui-etu@etu.univh2c.ma (S. El Harfaoui), ali.mouhssine-etu@etu.univh2c.ma (A. Mohssine), anas.driouich-etu@etu.univh2c.ma (A. Driouich), khalid.digua@univh2c.ma (K. Digua), hassan.chaair@univh2c.ma (H. Chaair)*
[b]*Laboratory of Advanced Materials and Process Engineering, Faculty of Sciences, University Ibn Tofail, BP 242, Kenitra, Morocco, emails: zakia.zmirli@iut.ac.ma (Z. Zmirli), brahimsallek@gmail.com (B. Sallek)*

Received 10 October 2022; Accepted 7 March 2023

ABSTRACT

The present paper focuses on the treatment of indigo blue dye from an industrial wastewater using coagulation–flocculation process and explains removal mechanisms through the density functional theory. The conducted study analyzed the effect of different factors, including the dose and concentration of the coagulant $AlCl_3$, flocculant dose, and pH and their influence on coloration removal, chemical oxygen demand (COD) reduction, and sludge amount, and seeks the optimization of these factors using the design of experiment. The optimal removal efficiencies were found to be 96.42% for COD, 98.21% for absorbance, and 10.40 mL for sludge volume under optimal operational parameters, 11.25, 4.07 mL, 3.23 g/L, and 0.94 mL for pH, coagulant dose, concentration dose, and flocculant dose with a total cost of 0.0826 USD/m^3, respectively. Analysis of the global reactivity descriptors for reagents indicated that $AlCl_3$ (ω = 6.156 eV) acts as an electrophile and the indigo blue dye (ω = 7.174 eV) as a nucleophile. The Parr's index analysis P_k^+ and P_k^- of indigo blue revealed that the vulnerable location for the nucleophilic attack is sited on the $-C_8=O_{10}$ and $-C_{11}=O_{19}$ bonding area. Finally, the developed model may emphasize the process engineering aspects of industrial wastewater treatment, and the linking with theoretical data could explain the involved removal mechanisms.

Keywords: Indigo dye; Wastewater treatment; Design of experiment (DOE); Analysis of variance; Modelization; Density functional theory (DFT)

1. Introduction

The worldwide dyes production is estimated at 700,000 tons/y of which azo dyes represent 60%–70% [1–3]. Significant amounts of dyes are lost during the manufacturing and application processes [4], and nearly 0.28 million tons are randomly discharged into the environment [5,6] generating harmful impacts. The textile industry is widely regarded as the most polluting of all industrial sectors, producing around 54% of colored effluents [7]. The decolorization of textile and dyestuff manufacturing effluents remains a major environmental concern.

The most employed dye in the textile industry is indigo blue [8,9] which is frequently used to dye denim and employed as a coloring element in a multitude of applications [10,11]. This dye is known by the existence of a water-insoluble ketonic group (C=O). However, its chemical structure may change into a simplified form (C–OH), a Leucoindigo, soluble in water with a chemical preference

* Corresponding author.

for cellulose fibers, when sodium dithionite is present in an alkaline solution ($Na_2S_2O_4$) [12]. On average, it's estimated that dyeing a denim blue pants needs 3 to 12 g of indigo [4]. As a result, the industry of washing and dyeing textiles is one of the primary contributors to indigo dye contamination in the environment. Because of its composition, the complexity of its aromatic structure (Fig. 1) [13], and natural stability [8], indigo blue is difficult to treat, causing serious environmental pollution [7,14–17]. Even at low concentrations, indigo blue could have harmful impacts on all living being and become a serious concern due to its non-biodegradable character in nature. In fact, the efficacy of indigo treatment relies on the accurate control of the main influencing parameters, namely pH [18], dyes structures [16], doses, and type of coagulant and flocculant [19].

To solve ecological and toxicological concerns related to the application of indigo blue dye dyestuff, various dye removal techniques have been documented [13]. The widely used methods for dyeing wastewater treatment involve several techniques, such as coagulation [12,19] electrocoagulation [20–23], coagulation and electrocoagulation [24,25], adsorption/ultrafiltration system [26,27], membrane filtration [28], advanced oxidation [29], ozonation [30], radiation-induced cationic hydrogel's [31], biological treatment [32] or combined processes, etc. Each treatment method has its advantages and disadvantages [18] and final results fluctuate depending on the used process.

For that reason, there is an urgent need for more effective dye removal treatment technology, as well as the control of influencing parameters. Coagulation–flocculation treatment can be used to effectively remove indigo dye and has been frequently employed in the past as an efficient and affordable process, with wider availability, and ease of application, sustainable technology with promising potential to treat various wastewater types, especially in developing countries, as shown in previous studies [33–36]. The main advantage of the coagulation–flocculation method is that the textile wastewater can be decolorized through the removal of dye molecules from the effluents, and not by partial decomposition of dyes, which could produce potentially harmful and toxic aromatic compounds [37]. Generally, coagulation–flocculation is a common wastewater treatment technique that requires a large number of experiments to optimize the working parameters. To overcome this constraint, response surface methodology (RSM), a multivariate optimization technique, has been demonstrated as a modeling technique for optimizing coagulation–flocculation conditions [38–43].

Therefore, this study is a synergistic approach between the use of density functional theory (DFT) to explain the reaction mechanism between indigo dye and $AlCl_3$ coagulant; and mathematical modeling in the form of a response surface methodology as an optimization methodology.

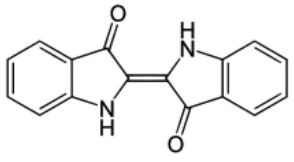

Fig. 1. General structure of indigo dye [13].

Hence, the originality of this work consists in developing a theoretical and experimental model to control the process of industrial wastewater treatment.

The present work focuses on the model development for treating the industrial wastewater (case of effluent containing indigo blue dye) in a perfectly stirred continuous flow reactor by coagulation process and optimizes influencing parameters using an orthogonal central composite design (CCD). Furthermore, through using the density functional theory (DFT), we emphasize chemical interactions between the reagent aluminum chloride ($AlCl_3$) and indigo blue dye and we describe the action mode between the effluent and the coagulant by identifying the most vulnerable locations to nucleophilic attacks.

2. Materials and methods

2.1. Characterization of the effluent

The wastewater provides from the textile washing industry. According to the Standard Methods for the Examination of Water and Wastewater, the samples were taken and stored [44]. The major properties of raw textile wastewater are listed in Table 1.

The chemical formula of indigo blue is $C_{16}H_{10}N_2O_2$, and it has a molecular weight of 262.26 g/mol and an absorbed wavelength of around 665 nm. Fig. 1 displays the general structure of the indigo blue dye.

2.2. Experimental methodology

The coagulation process is carried out to treat textile blue indigo effluent in a perfectly stirred continuous flow reactor (STCFR) (Fig. 2). The real industrial waste of indigo blue is regularly injected into the reactor, with a volume of 5 L. The STCFR consists of a tank that is cylindrical with a convex bottom, internal diameter D = 20.6 cm, and ratio H/D = 0.73, equipped with a 6 cm diameter marine propeller placed at 6 cm in the bottom up to prevent decantation. To guarantee proper mixing, the mixing speed is set at 300 rpm. The pH of the real reject is regulated to the

Table 1
Characterization of the textile effluent used in this study

Physico-chemical characteristics	Value of the raw textile wastewater	Disposal limits values (*)
Chemical oxygen demand, mg/L	3,690 ± 65.42	900
Absorbance	0.247 ± 0.003	–
Turbidity, NTU	132 ± 4.5	–
Conductivity, mS/cm	14.664 ± 3.6	–
pH	7.5 ± 0.2	5.5–8.5
Temperature, °C	22 ± 2	30
Total suspended solids (TSS), mg/L	753.33 ± 43.37	400
Color	Indigo blue	–
Toxicity	**Category GHS08**	–

(*) For Morocco [45].

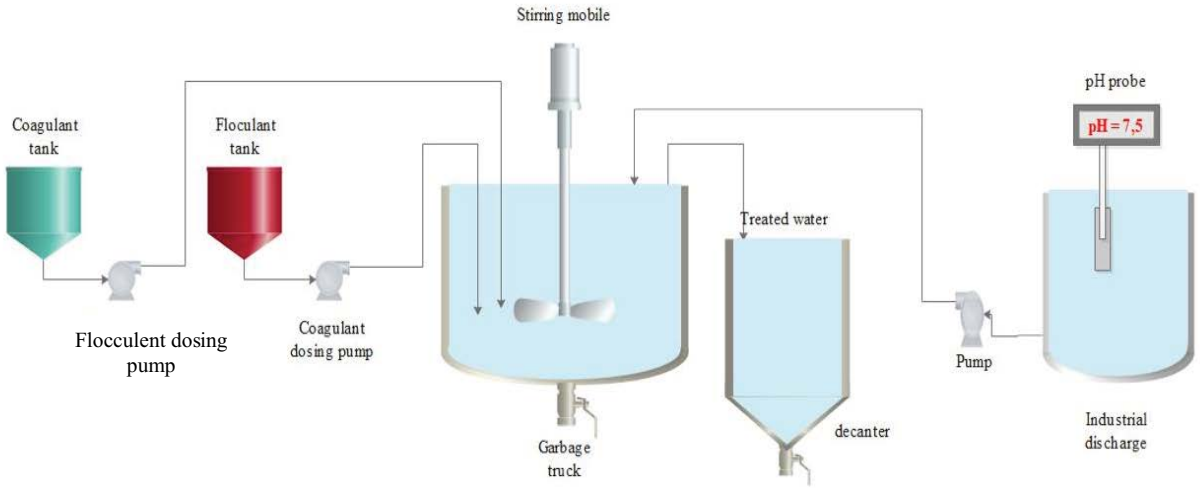

Fig. 2. Schematic diagram of the experimental.

desired value using NaOH or H_2SO_4 with maximum purity (purchased from Sigma-Aldrich Chemie Co., Germany) and measured using Accumet Basic (AB15 pH-meter).

To prepare every solution in this investigation, distilled water was utilized. The coagulant solution is prepared using $AlCl_3$ powder as a coagulant (purchased from Sigma-Aldrich, Germany), and the flocculant used is Himoloc DR3000 (purchased from Derypol, S.A., Spain). Table 2 shows a summary of aluminum chloride's properties, and HIMOLOC DR 3000. HIMOLOC DR 3000 is the commercial name of the flocculant compound used. HIMOLOC DR 3000 is purchased from Derypol, S.A. The desired flow rate, flocculant, and coagulant are performed. The pollutant from the coagulation process unit is sampled. The steady-state operation is attained after 30 min. The materials are decanted and filtered using commercial paper filtration [46]. The supernatant was then recovered and examined to determine the percentage of chemical oxygen demand (COD) removed using a spectrophotometer type HACH-LANGE DR 3900 (Germany) apparatus and absorbance by spectrophotometer Type U-5100 UV/VIS (Hitachi, Japan) apparatus, and at the end, the reading of the of sludge volumes directly on a graduated settling cone.

As a first step, experiments were undertaken as a preliminary study to refine the range of possible results of coagulant dosage (CD), flocculant dosage (FD), the concentration of coagulant [coag], and pH before designing the experimental runs. The following formulas are used to calculate the COD removal percentage, absorbance, and recovered sludge volume.

2.2.1 % Removal COD calculations

The following formula [Eq. (1)] was used to calculate the response removal percentages (COD):

$$\%\text{Removal COD} = \frac{\left(\text{COD}_i - \text{COD}_f\right)}{\text{COD}_i} \times 100 \quad (1)$$

where COD_i and COD_f represent the response COD's initial and final values, respectively [42].

Table 2
Characteristics of the coagulant and flocculant used in the study

	Aluminum chloride	Himoloc DR3000
Appearance	Light yellow solid	White milky liquid
Density, g/cm^3	2.48	~1.2
Viscosity	0.35	<600 cp
pH	9–11	3.0–4.1
Molecular weight, g/mol	133.341	High

2.2.2. Color removal (%)

The color removal efficiency (dye removal) was calculated using the following formula Eq. (2) and computed from absorbance before (without treatment) and after treatment [34,46–48]. The absorbances were performed at the maximum wavelength λ_{max} of 664 nm ($660 \le \lambda_{max} < 666$) using a spectrophotometer of the Type U-5100 UV/VIS (Hitachi, Japan) apparatus.

$$\text{Color removal}(\%) = \frac{\left(\text{Abs}_0 - \text{Abs}\right)}{\text{Abs}_0} \times 100 \quad (2)$$

where Abs_0 and Abs represent the initial and final absorbances of the sample, respectively.

The UV-Visible spectrum of the raw water (Fig. 3) shows that a maximum is obtained for absorbances between 660 and 666 nm.

2.2.3. Sludge volume

The direct reading on a graduated settling cone was taken to determine the sludge volume (mL).

2.2.4. Treatment cost calculations

The average cost of effluent treatment ($/m^3) at the laboratory scale is estimated based on the cost of raw materials

coagulant (Q_c), flocculant (Q_f), and NaOH (Q_a). Labor costs, energy consumption, and sludge treatment were not considered. The average cost per m^3 is calculated by the following equation [Eq. (3)]:

$$\text{Cost}\left(\$/\text{m}^3\right) = P_c Q_c + P_f Q_f + P_a Q_a \quad (3)$$

where Q_c: quantity coagulant used per m^3 wastewater treated; Q_f: quantity flocculant used per m^3 wastewater treated; Q_a: quantity NaOH used per m^3 wastewater treated; P_c: price of coagulant (\$/kg); P_f: price of flocculant (\$/kg); P_a: price of NaOH (\$/kg).

The cost of 1 kg $AlCl_3$ = 13.816 USD, 1 kg flocculant = 4 USD, and 1 kg NaOH = 14 USD, cost (\$/m^3) = 0.0826 USD/m^3.

2.3. Computational details via quantum chemical studies by DFT

In this work, the application of density functional theory (DFT/B3LYP) with a 6–31G basis set using Gaussian 09W software [49,50] was performed to explain the reaction mechanism of indigo blue removal by $AlCl_3$ in an alkaline environment. This theoretical evaluation was focused on the nucleophilic attack and the identification of the active sites of indigo blue dye.

The most common variables that have a significant impact on chemical reactivity are the eigenvalues of the energy of the highest occupied molecular orbital (E_{HOMO}), the energy of the lowest unoccupied molecular orbital (E_{LUMO}), energy gap (ΔE_{gap}), ionization energy (IE), electron affinity (EA), absolute electronegativity (χ), global hardness (η), global softness (S), global electrophilicity index (ω), the electroaccepting, ω^+, and electrodonating, ω^-. The HOMO and LUMO energies were used to calculate the global indexes described in the framework of the DFT, they are utilized in chemical processes as descriptors. The following expressions were used to estimate these values [51,52]:

(E_{HOMO}): highest occupied molecular orbital,

(E_{LUMO}): energy of the lowest unoccupied molecular orbital,

ΔE_{gap} (eV) = $E_{LUMO} - E_{HOMO}$,

Electronic chemical potential: $\mu = \dfrac{E_{LUMO} + E_{HOMO}}{2}$

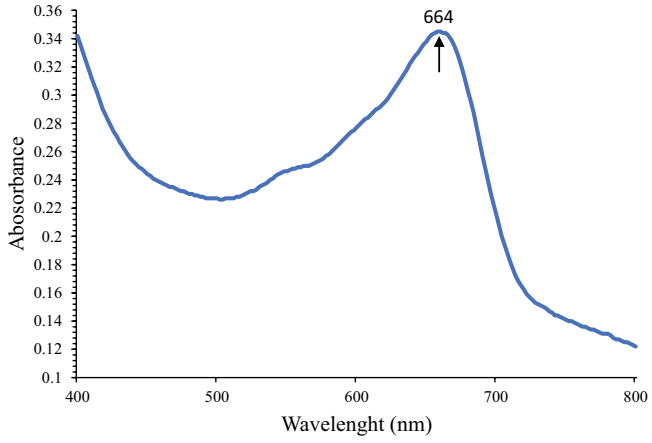

Fig. 3. UV-Vis spectrum of raw water.

Electrophilicity index: $\omega = \dfrac{\mu^2}{2} \times S = \dfrac{\mu^2}{2\eta}$

Absolute chemical hardness: $\eta = \dfrac{\text{IE} - \text{AE}}{2} = \dfrac{E_{LUMO} - E_{HOMO}}{2}$

Chemical softness: $S = \dfrac{1}{\eta} = \dfrac{2}{E_{HOMO} - E_{LUMO}}$

Electroaccepting: $\omega^+ = \dfrac{\text{EA}^2}{2\left(\text{IE} - \text{EA}\right)}$

Electrodonating: $\omega^- = \dfrac{\text{IE}^2}{2\left(\text{IE} - \text{AE}\right)}$

Ionization energy: IE = $-E_{HOMO}$

Electron affinity: EA = $-E_{LUMO}$

N: empirical nucleophilic index based on HOMO energies.

2.4. Design of experiments

2.4.1. Definition of experimental field

To carry out this study, a choice of the domain of variation for each factor is very crucial. In this experimental field, two elements must be taken into consideration [46]:

- The range of factors fluctuation must be sufficiently wide to show significant response variations;
- It must be sufficiently constrained to be able to model the variations that may happen in an uncontrolled way while the method is being used.

Hence, based on initial investigations, the experimental domain for the four parameters chosen has been defined. The following ranges for good treatment were revealed by preliminary laboratory tests (Table 3). Each parameter was assigned a code at five levels: (–1) for the lowest level, (0) for the middle level, (+1) for the highest level, and –2 and +2 for the extreme level. Table 3 shows the factors chosen as well as their experimental domain.

According to Eq. (4), the coded variables are computed as follows:

$$X_i = \frac{\left(x_i - x_0\right)}{\Delta x_i} \quad (4)$$

where X_i is the non-dimensional value of an independent factor, x_i is the real value of an independent parameter, x_0 is the value of x_i at the center point, and Δx_i is the step range.

Table 3
Natural and coded factors used in the experimental design

Natural variable (x_i)	Coded factors X_1, X_2, X_3, X_4				
	–α	–1	0	+1	+α
x_1 = pH	6	7.5	9	10.5	12
x_2 = coagulant dose, mL	2.25	2.75	3.25	3.75	4.25
x_3 = coagulant concentration, g/L	1	2	3	4	5
x_4 = flocculant dose, mL	0.5	0.75	1	1.25	1.5

2.4.2. Design of the experiment and data analysis

Two programs, JMP PRO version 16.0 Software (SAS) [53] and Stat Soft STATISTICA 12 [54], were used to plan the experiments and perform the statistical analysis of the data. In this study, the four most important operating parameters (coagulant dosage, flocculant dosage, concentration dose, and pH) were optimized using the orthogonal central composite design (CCD) [55]. Analysis of variance (ANOVA) was evaluated statistically using the Fisher test (*F*-test) and a probability (*p*-value) of 0.05 [56]. The model validation was also evaluated using the determination coefficient R^2, which was completed by analyzing the computed values to the expected values.

2.4.2.1. Orthogonal central composite design

An orthogonal central composite design was applied to analyze empirical data correlations between the three responses, % COD, % absorbance, pH, and the four factors reported in Table 3 that affect the treatment of industrial waste. Table 3 displays the levels related to each variable.

In this design, there are three different kinds of points: cube points derived via factorial design (2^k), axial points ($2k$) carried out on the axis at a distance of ±α from the center (N_a), and central points (N_0). To achieve orthogonality, the distance α is computed. Eqs. (5) and (6), respectively, provide the experiment number (N) and the distance α.

$$N = N_f + N_a + N_0 = 2^k + 2K + N_0 \tag{5}$$

$$\alpha = 2^k - \left(\frac{\left(2^k + 2\alpha^2\right)^2}{n} \right) = 0 \tag{6}$$

$$\alpha = \pm 2$$

where $k = 4$ denotes the number of parameters.

N_0 experiments are conducted in the middle of the experimental range. In our case, the N_0 value was set at 12 to achieve orthogonality. The experiments performed at the domain's center (36–24) in Table 4 result in an independent estimation of the 'pure' experimental error variance.

Considering that this study uses four factors (k = 4), the number of experiments could be split into three categories as follows: $2^k = 2^4 = 16 = N_f$ factorial experiments, $2k = 2 \times 4 = 8 = N_a$ axial experiments, and $N_0 = 12$ central experiments.

The experimental matrix displayed in Table 4 is a Hadamard matrix made up of 36 experiments, based on the combinations selected using orthogonal central composite design (CCD).

2.4.2.2. Mathematical pattern

Using a quadratic polynomial equation, the dependent variables were modeled using the second-order equation [Eq. (7)]:

$$Y_i = b_0 + \sum_{i=1}^{k} b_i X_i + \sum_{i=1}^{k} b_{ii} X_i^2 + \sum_{i}^{i<j} \sum_{j} b_{ij} X_i X_j + \varepsilon \tag{7}$$

where Y_i is the response variable that needs to be modeled, X_i and X_j are the independent variables influencing Y; and b_0, b_i, b_{ii}, b_{ij}, and ε are the offset terms, the ith linear coefficient, the quadratic coefficient, their interaction coefficient, and residue, respectively.

3. Results and discussions

3.1. Statistical analysis

3.1.1. Regression variance analysis

The continuous coagulation–flocculation process was modeled and optimized using the response surface method (RSM) in combination with the orthogonal central composite design (OCCD). The analysis of variance (ANOVA) is used to assess the quality of the regression using some statistical tools such as *F*-ratio, *p*-values, and determination coefficient (R^2) [46,56–60].

Table 5 indicates that the F_{exp} ratio calculated experimentally (F_{exp}) is equivalent to 26.8209, 21.7546, and 44.8387, respectively, for COD, absorbance, and sludge volume responses which is greater than the value of the critical Fisher–Snedecor factor for a confidence level of 95%, and the corresponding degrees of freedom associated to model and residual variances equal to 14 and 21 ($F_{0.05}$ (14, 21) = 2.22). The corresponding *p*-values is strictly lower than the level of significance α (α = 0.05), which implies that the *F*-ratio is statistically significant. Consequently, we can say that the model's components are quite important with p-values of regression being strictly less than 0.05 (*p*-value = < 0.0001).

3.1.2. Graphical representation of factor effects

The effects of varying the pH range 6–12, coagulant dose 2.25–4.25 mL, coagulant concentration 1–5 g/L, and flocculant dose 0.5–1.5 mL on treatment performance were evaluated (Fig. 3).

3.1.2.1. Factors effects on % COD removal, absorbance

Fig. 4 shows the estimated response profiles of % absorbance (a), % COD (b), and sludge volume (c), which vary as the setting of individual factors changes. According to Fig. 4a and b it was concluded that:

- The studied variables have approximatively the same effects on % COD and decolorization (% absorbance): When the value of the pH factor rises from a lower value (pH = 6) to a higher one (pH = 12), the response % COD and % absorbance value increase also 78.82% to 92.30% and 81.78% to 92.87% for % COD and % absorbance, respectively, this suggests that the pH factor influences the response positively. Additionally, it is clear from these data that in a basic medium, as opposed to an acidic one, COD removal efficiency and percent absorbance are more significant. Also, it may be concluded that the sweep-floc process and dye molecule trapping play a major role in floc generation at alkaline pH. Accordingly, larger flocs are produced, which results in the simultaneous precipitation of dye compounds and flocs at basic pH. Similar observations have been reported by [62].

Table 4
Experimental matrix based on an orthogonal central composite design

Order		Configuration	pH		Coagulant dose (mL)		Concentration dose (g/L)		Flocculant dose (mL)	
Logical order	Randomized order		X_1	x_1	X_2	x_2	X_3	x_3	X_4	x_4
1	3	− − − −	–1	7.5	–1	2.75	–1	2	–1	0.75
2	22	− − − +	–1	7.5	–1	2.75	–1	2	1	1.25
3	8	− − + −	–1	7.5	–1	2.75	1	4	–1	0.75
4	1	− − + +	–1	7.5	–1	2.75	1	4	1	1.25
5	10	− + − −	–1	7.5	1	3.75	–1	2	–1	0.75
6	26	− + − +	–1	7.5	1	3.75	–1	2	1	1.25
7	16	− + + −	–1	7.5	1	3.75	1	4	–1	0.75
8	20	− + + +	–1	7.5	1	3.75	1	4	1	1.25
9	34	+ − − −	1	10.5	–1	2.75	–1	2	–1	0.75
10	2	+ − − +	1	10.5	–1	2.75	–1	2	1	1.25
11	5	+ − + −	1	10.5	–1	2.75	1	4	–1	0.75
12	18	+ − + +	1	10.5	–1	2.75	1	4	1	1.25
13	19	+ + − −	1	10.5	1	3.75	–1	2	–1	0.75
14	15	+ + − +	1	10.5	1	3.75	–1	2	1	1.25
15	29	+ + + −	1	10.5	1	3.75	1	4	–1	0.75
16	4	+ + + +	1	10.5	1	3.75	1	4	1	1.25
17	25	–α 0 0 0	–2	6	0	3.25	0	3	0	1
18	28	+α 0 0 0	2	12	0	3.25	0	3	0	1
19	24	0 –α 0 0	0	9	–2	2.25	0	3	0	1
20	14	0 +α 0 0	0	9	2	4.25	0	3	0	1
21	9	0 0 –α 0	0	9	0	3.25	–2	1	0	1
22	12	0 0 +α 0	0	9	0	3.25	2	5	0	1
23	36	0 0 0 –α	0	9	0	3.25	0	3	–2	0.5
24	17	0 0 0 +α	0	9	0	3.25	0	3	2	1.5
25	6	0 0 0 0	0	9	0	3.25	0	3	0	1
26	11	0 0 0 0	0	9	0	3.25	0	3	0	1
27	7	0 0 0 0	0	9	0	3.25	0	3	0	1
28	13	0 0 0 0	0	9	0	3.25	0	3	0	1
29	21	0 0 0 0	0	9	0	3.25	0	3	0	1
30	27	0 0 0 0	0	9	0	3.25	0	3	0	1
31	23	0 0 0 0	0	9	0	3.25	0	3	0	1
32	35	0 0 0 0	0	9	0	3.25	0	3	0	1
33	32	0 0 0 0	0	9	0	3.25	0	3	0	1
34	30	0 0 0 0	0	9	0	3.25	0	3	0	1
35	33	0 0 0 0	0	9	0	3.25	0	3	0	1
36	31	0 0 0 0	0	9	0	3.25	0	3	0	1

X_i: Coded factor; x_i: Real factor, $\alpha = \pm 2$.

- The coagulant and flocculant doses have a slight effect on % COD elimination and % absorbance when their doses in (mL) are lower than 3.45 mL coagulant dose and 1 mL for flocculant dose. Above these values, the result showed that an increase in both coagulant dosage and initial coagulant concentration increases the percentage of dye removal and COD abatement;
- Also, it was observed that as the dosing quantity of coagulant, $AlCl_3$ is increased up to a maximum dose of about 3.5 g/L the removal efficiency is enhanced for the COD and % absorbance; from this dose (3.5 g/L) the COD and absorbance removal percentages showed a significant drop due to excessive addition of coagulant.

3.1.2.2. Factors effects on sludge volume

Fig. 4c illustrates the estimated sludge volume response profile as a function of the investigated factors. As could be

Table 5
Results of the analysis of variance

Source	Degree of freedom	Sum of squares	Mean square	F_{exp}	p-value	Significance
For chemical oxygen demand response						
Model	14	489.5047	34.9646	26.8209	<0.0001	***
Residual	21	27.3762	1.3036			
Total	35	516.8809				
R square	0.95					
R square adjusted	0.91					
For absorbance response						
Model	14	369.1471	26.3677	21.7546	<0.0001	***
Residual	21	25.4530	1.2120			
Total	35	394.6001				
R square	0.94					
R square adjusted	0.89					
For sludge volume response						
Model	14	249.80924	17.8435	44.8387	<0.0001	***
Residual	21	8.35692	0.3979			
Total	35	258.16616				
R square	0.97					
R square adjusted	0.95					

***: significant at a level of 0.1% ($F_{0.001}$ (14, 21) = 4.48) [61].

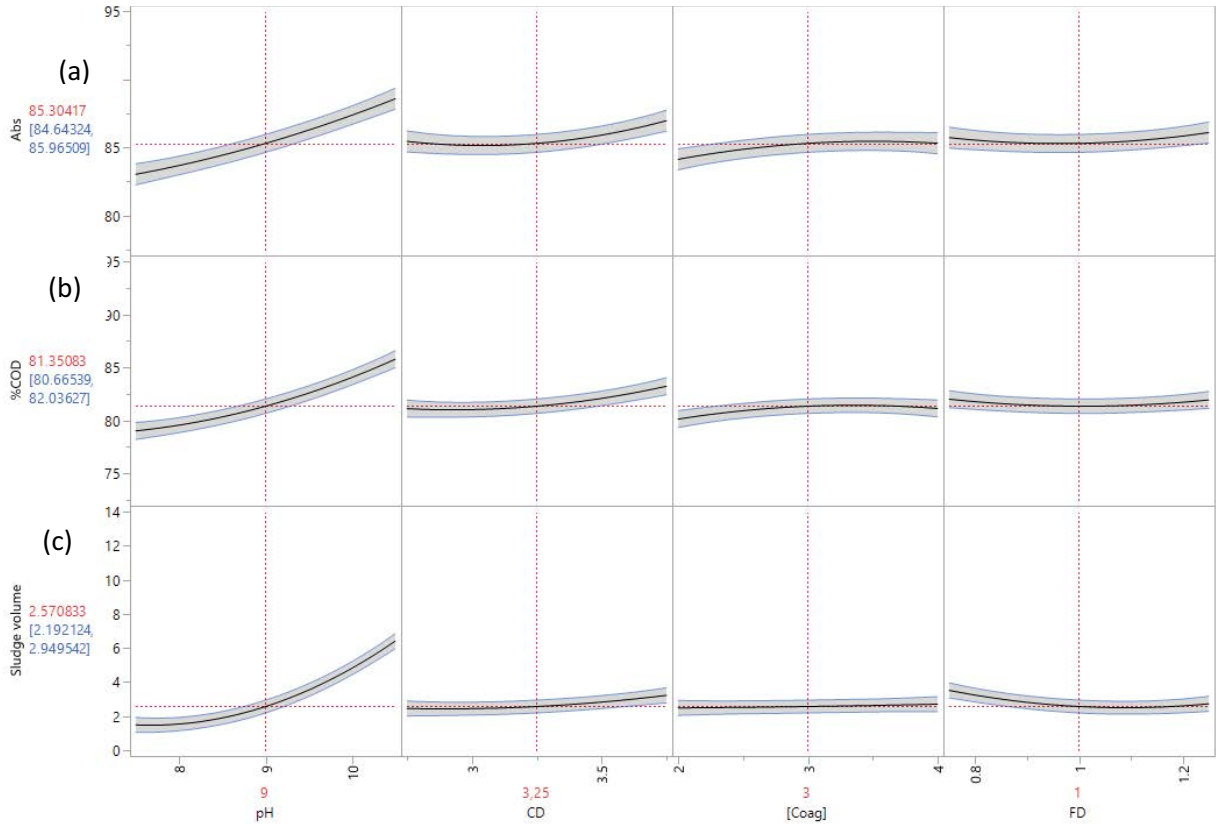

Fig. 4. Main effects of factors on (a) % absorbance (Abs), (b) % chemical oxygen demand removal, and (c) sludge volume responses. Where: CD: coagulant dose; FD: flocculant dose; [coag]: concentration of coagulant.

seen in this figure, the sludge volume yield is more important in a basic medium than in an acidic medium. According to Fig. 4c, it was concluded that:

- As the pH factor value rises from a minimum to a maximum, the sludge volume value reduces slightly and increases in the basic medium;
- Sludge production falls while coagulant doses are increased, then increases;
- The concentration of the coagulant used has a slight effect on the amount of sludge recovered;
- The amount of sludge denotes the maximum removal rate at a low flocculant dose, then rapidly decreases. The existence of dense flocs, which occupy less volume, can explain the proportion of sludge drop and low volume recorded as the flocculant dose was increased.

3.1.3. Statistical evaluation of the effects of factors

Table 6 displays the estimated regression coefficients for % COD removal, *F*-values, and *p*-values for all linear, quadratic, and interaction effects of the parameters. In Table 6, it should be emphasized that the linear influence of pH, CD, and [coag], interaction effects pH × CD, pH × [coag], CD × [coag], CD × FD, pH × FD, and the quadratic effect pH^2, CD^2, $[coag]^2$ and FD^2 are very significant. The *p*-value for all linear and interaction effects is 0.05, whereas the *p*-value for quadratic effects is $pH^2 < 0.0001$. The linear effect of FD is not significant (*p*-values > 0.05).

Additionally, the most important factor is pH, followed by the interaction CD × FD and pH^2 with an *F*-value equal to 210.42, 28.68, and 27.24, respectively. The significant model terms for % COD removal is listed in the following order according to the *F*-values:

pH > CD × FD > pH^2 > CD > CD^2 > CD × [coag] > pH × CD > $[coag]^2$ > pH × [coag] > FD^2 > [coag] > pH × FD > [caog] × FD. This study supports COD removal effectiveness as a function of pH (with F_{exp} = 210.42 and estimate coefficient = 3.38). Similar findings were reported by [63], which validated the current result.

Likewise, Table 7 displays the computed regression coefficients and related *F* and *P* values for absorbance for treated effluent. It's noted that all linear effects, quadratic effects, and interactions are critical parameters (*p*-value < 0.01) except linear effect FD and interaction pH × FD are not significant. According to *F*-values (*F*-value = 152.02, estimated coefficient = 2.7708), pH is the most important parameter. Based on *F*-values for the absorbance, the order of significant factors is as follows:

pH > CD × FD > CD^2> pH × CD > pH × [coag] > CD > CD × [coag] > FD > $[coag]^2$ > [coag] > pH^2 > [coag] × FD. As a result, the term pH defines and influences absorbance.

Furthermore, Table 8 displays that some coefficients have a positive impact on the sludge volume response while others have a negative effect, except for the linear effect [coag], interaction effect pH × [coag], and quadratic effect $[coag]^2$ which had no significant effect. Also, the term pH is the parameter influencing the amount of sludge.

3.2. Analysis of the Pareto diagram

The Pareto diagram is employed to pinpoint the 20% of the variables and interactions that exhibit an 80% treatment impact on textile wastewater containing indigo blue dye.

The results of the Pareto diagram (Fig. 5) clearly show that pH, interaction coagulant dose × flocculant dose, coagulant dose × concentration dose, coagulant dose, quadratic effect pH × pH, interaction pH × coagulant dose,

Table 6
Estimation regression coefficients for chemical oxygen demand response

Source	Estimated coefficient	Standard error	Sum of squares	F_{exp}	*p*-value	Significance
Constant	81.350833	0.3296	–	–	–	–
pH	3.3808333	0.233062	274.32082	210.4280	<0.0001	***
CD	1.0575	0.233062	26.83935	20.5881	0.0002	***
[coag]	0.5	0.233062	6.00000	4.6025	0.0438	*
FD	–0.034167	0.233062	0.02802	0.0215	0.8848	NS
pH × CD	1.02875	0.285442	16.93323	12.9893	0.0017	**
pH × [coag]	–0.88375	0.285442	12.49623	9.5857	0.0055	**
CD × [coag]	1.12375	0.285442	20.20503	15.4990	0.0008	***
pH × FD	0.57875	0.285442	5.35923	4.1110	0.0555	NS
CD × FD	–1.52875	0.285442	37.39323	28.6839	<0.0001	***
[coag] × FD	0.48625	0.285442	3.78302	2.9019	0.1032	NS
pH × pH	1.0535417	0.201838	35.51840	27.2457	<0.0001	***
CD × CD	0.8235417	0.201838	21.70307	16.6481	0.0005	***
[coag] × [coag]	–0.717708	0.201838	16.48337	12.6442	0.0019	**
FD × FD	0.6235417	0.201838	12.44173	9.5439	0.0056	**

***: significant at a level of 0.1% ($F_{0.001}$ (1,21) = 14.59);
**: significant at a level of 1% ($F_{0.01}$ (1,21) = 8.02);
*: significant at a level of 5% ($F_{0.05}$ (1,21) = 4.32 [61];
NS: no-significant.

Table 7
Estimation regression coefficients for absorbance response

Source	Estimated coefficient	Standard error	Sum of squares	F_{exp}	*p*-value	Significance
Constant	85.304167	0.317811	–	–	–	–
pH	2.7708333	0.224726	184.26042	152.0241	<0.0001	***
CD	0.7608333	0.224726	13.89282	11.4623	0.0028	**
[coag]	0.5891667	0.224726	8.33082	6.8733	0.0159	*
FD	0.1866667	0.224726	0.83627	0.6900	0.4155	NS
pH × CD	1.15375	0.275233	21.29822	17.5721	0.0004	***
pH × [coag]	–1.0325	0.275233	17.05690	14.0728	0.0012	**
CD × [coag]	0.91125	0.275233	13.28602	10.9616	0.0033	**
pH × FD	0.19375	0.275233	0.60062	0.4955	0.4892	NS
CD × FD	–1.69	0.275233	45.69760	37.7028	<.0001	***
[coag] × FD	0.65875	0.275233	6.94323	5.7285	0.0261	*
pH × pH	0.5058333	0.194619	8.18776	6.7553	0.0167	*
CD × CD	0.9045833	0.194619	26.18467	21.6037	0.0001	***
[coag] × [coag]	–0.581667	0.194619	10.82676	8.9326	0.0070	**
FD × FD	0.6058333	0.194619	11.74509	9.6903	0.0053	**

***: significant at a level of 0.1% ($F_{0.001}(1,21) = 14.59$);
**: significant at a level of 1% ($F_{0.01}(1,21) = 8.02$);
*: significant at a level of 5% ($F_{0.05}(1,21) = 4.32$; [61];
NS: no-significant.

Table 8
Estimation regression coefficients for sludge volume response

Source	Estimated coefficient	Standard error	Sum of squares	F_{exp}	*p*-value	Significance
Constant	2.5708333	0.182105	–	–	–	–
pH	2.4616667	0.128768	145.43527	365.4622	<0.0001	***
CD	0.385	0.128768	3.55740	8.9393	0.0070	**
[coag]	0.1108333	0.128768	0.29482	0.7408	0.3991	NS
FD	–0.394167	0.128768	3.72882	9.3701	0.0059	**
pH × CD	–0.50875	0.157708	4.14123	10.4064	0.0041	**
pH × [coag]	–0.22875	0.157708	0.83723	2.1039	0.1617	NS
CD × [coag]	0.34625	0.157708	1.91822	4.8203	0.0395	*
pH × FD	–0.74625	0.157708	8.91023	22.3904	0.0001	***
CD × FD	–0.34625	0.157708	1.91823	4.8203	0.0395	*
[coag] × FD	0.60875	0.157708	5.92923	14.8995	0.0009	***
pH × pH	1.3808333	0.111516	61.01442	153.3223	<0.0001	***
CD × CD	0.2708333	0.111516	2.34722	5.8983	0.0242	*
[coag] × [coag]	0.0270833	0.111516	0.02347	0.0590	0.8105	NS
FD × FD	0.5520833	0.111516	9.75347	24.5094	<0.0001	***

***: significant at a level of 0.1% ($F_{0.001}(1,21) = 14.59$);
**: significant at a level of 1% ($F_{0.01}(1,21) = 8.02$);
*: significant at a level of 5% ($F_{0.05}(1,21) = 4.32$; [61];
NS: no-significant.

pH × concentration dose, and quadratic effect coagulant dose represent 20% of parameters that have an 80% impact on "% the COD removal" response.

From Fig. 5, we concluded that these factors need to be checked to improve COD removal.

The outcomes of the Pareto diagram (Fig. 6) showed that pH, interaction coagulant dose × flocculant dose, pH × coagulant dose, pH × concentration dose, coagulant dose × concentration dose, quadratic effect coagulant dose, coagulant dose, and concentration coagulant × flocculant dose represent 20% of terms that have 80% impacts on the % absorbance. From Fig. 6, we concluded that these factors need to be managed to improve absorbance.

Also, the analysis in Fig. 7, showed that pH, quadratic effect pH, pH × flocculant dose, concentration dose × flocculant dose, quadratic effect flocculant dose, pH × coagulant

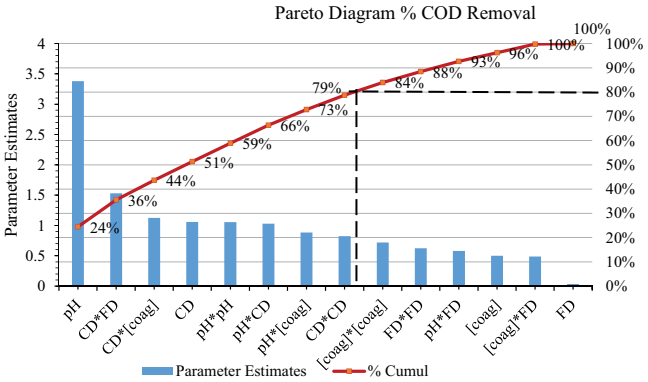

Fig. 5. Classification of factors effects and interactions on chemical oxygen demand removal according to Pareto diagram.

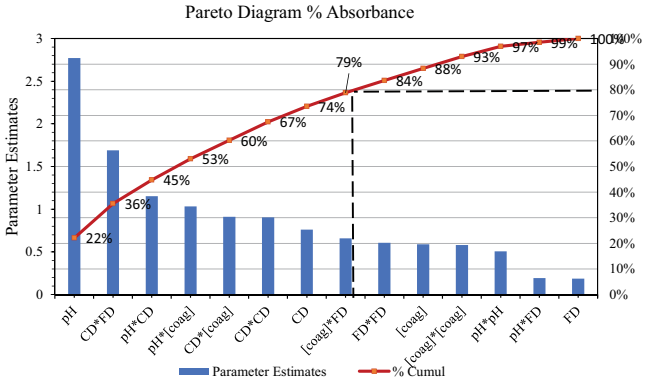

Fig. 6. Classification of factors effects and interactions on % absorbance according to Pareto diagram.

dose, and flocculant dose represent 20% of terms that have 80% effects on the sludge volume. From Fig. 7 we concluded that these factors need to be checked to reduce sludge volume.

For the three responses, we can say that to improve the elimination of indigo blue dye it is necessary to act on the pH, coagulant dose, and flocculant dose which have the most influence on the responses.

3.3. Modelization of COD removal, % absorbance, and sludge volume

JMP and statistical software were used to analyze and interpret the results of the experimental design to evaluate the reaction of the dependent variable throughout experiments.

The response functions of COD removal efficiency, absorbance (%), and sludge volume (mL). were fitted using regression analysis. Eqs. (8)–(10), respectively, express the final models in terms of coded parameters after removing the irrelevant terms for all responses. The positive sign, in these equations, indicates a synergistic impact, whereas the negative sign implies an antagonistic effect.

The coefficients of correlation and determination were used to assess the models' level of fit. Only significant model terms with a 5% level of confidence and their estimated coefficients are considered in these equations. Because of

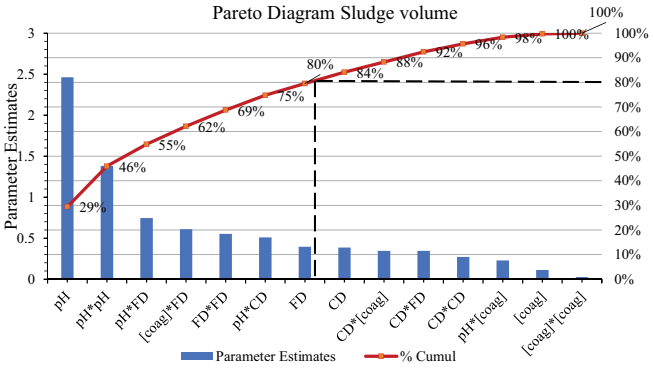

Fig. 7. Classification of factors effects and interactions on sludge volume according to Pareto diagram.

the very close near the standard error of their estimators (Tables 6–8) (varying from 0.2018 to 0.3296, 0.1946 to 0.3178, and from 0.1115 to 0.1821 for COD removal, % absorbance, and the sludge volume, respectively, these three models — Eqs. (8)–(10) — provide for the interpretation of the variation's variables and their relationships.

% COD removal response models (Y_1):

$$\begin{aligned}\text{COD} = {} & 81.35 + 3.38\text{pH} + 1.05\text{pH}^2 + 0.82\text{CD}^2 \\ & - 0.71\left[\text{coag}\right]^2 + 0.62\text{FD}^2 - 1.53\left(\text{CD}\times\text{FD}\right) \\ & + 1.12\left(\text{CD}\left[\text{coag}\right]\right) + 1.05\text{CD} + 1.02\left(\text{pH}\times\text{CD}\right) \\ & - 0.08\left(\text{pH}\left[\text{coag}\right]\right) + 0.5\left[\text{coag}\right] + 0.5\left(\text{pH}\times\text{FD}\right) \\ & + 0.48\left(\left[\text{coag}\right]\text{FD}\right)\end{aligned} \tag{8}$$

Absorbance removal models (Y_2):

$$\begin{aligned}\%\text{Absorbance} = {} & 85.3 + 2.77\,\text{pH} + 0.76\text{CD} + 0.51\text{pH}^2 \\ & + 0.94\text{CD}^2 - 0.58\left[\text{coag}\right]^2 + 0.60\text{FD}^2 + 0.58\left[\text{coag}\right] \\ & + 1.15\left(\text{pH}\times\text{CD}\right) - 1.03\left(\text{pH}\left[\text{coag}\right]\right) + 0.91\left(\text{CD}\left[\text{coag}\right]\right) \\ & - 1.69\left(\text{CD}\times\text{FD}\right) + 0.65\left(\left[\text{coag}\right]\text{FD}\right)\end{aligned} \tag{9}$$

Sludge volume generation models (Y_3):

$$\begin{aligned}\text{Sludge volume} = {} & 2.57 + 2.46\text{pH} - 0.39\text{FD} + 0.38\text{CD} \\ & + 1.38\text{pH}^2 + 0.55\text{FD}^2 + 0.27\text{CD}^2 0.74\left(\text{pH}\times\text{FD}\right) \\ & + 0.6\left(\left[\text{coag}\right]\text{FD}\right) - 0.51\left(\text{pH}\times\text{CD}\right) + 0.34\left(\text{CD}\left[\text{coag}\right]\right) \\ & - 0.34\left(\text{CD}\times\text{FD}\right)\end{aligned} \tag{10}$$

3.4. Model validation

Table 9 displays the predicted values, observed outcomes, and their residuals obtained using the statistical software JMP 11 [53]. Thus, when considering the experimental inaccuracy (residual), the assessment of these findings reveals that there is no statistically significant difference between the experimental and projected values, proving the validity of the existing models.

The relationship between expected and experimental values are displayed in Fig. 8a–c. We can see from this curve

Table 9
Residuals, experimental and predicted values for chemical oxygen demand removal, absorbance, and sludge volume

Standard run	Absorbance (%)			% Chemical oxygen demand			Sludge volume (mL)		
	Experimental	Expected	Residual	Experimental	Expected	Residual	Experimental	Expected	Residual
1	82.57	82.6263	–0.0562	79.89	79.0346	0.8554	1.6	1.3633	0.2367
2	85.8	84.6746	1.1254	80.23	79.8938	0.3363	1.9	1.5425	0.3575
3	83.99	82.7296	1.2604	79.56	78.5821	0.9779	1.06	0.1325	0.9275
4	87.42	87.4129	0.0071	80.98	81.3863	–0.4063	2	2.7467	–0.7467
5	84.19	83.3979	0.7921	80.21	79.9021	0.3079	3	3.1508	–0.1508
6	78.59	78.6863	–0.0963	74.67	74.6463	0.0238	2.8	1.945	0.855
7	86.21	87.1463	–0.9363	83.76	83.9446	–0.1846	3.5	3.305	0.195
8	84.19	85.0696	–0.8796	80.08	80.6338	–0.5538	3.9	4.5342	–0.6342
9	88.47	87.5379	0.9321	84.38	84.3488	0.0313	10	9.2542	0.7458
10	91.07	90.3613	0.7088	87.76	87.5229	0.2371	6.5	6.4483	0.0517
11	83.38	83.5113	–0.1313	80.39	80.3613	0.0288	6.5	7.1083	–0.6083
12	88.23	88.9696	–0.7396	84.65	85.4804	–0.8304	7	6.7375	0.2625
13	92.69	92.9246	–0.2346	89.79	89.3313	0.4588	10	9.0067	0.9933
14	87.78	88.9879	–1.2079	84.89	86.3904	–1.5004	4	4.8158	–0.8158
15	91.47	92.5429	–1.0729	88.98	89.8388	–0.8587	8	8.2458	–0.2458
16	91.07	91.2413	–0.1713	88.04	88.8429	–0.8029	6.5	6.49	0.01
17	81.09	81.7858	–0.6958	77.89	78.8033	–0.9133	2.83	3.1708	–0.3408
18	93.74	92.8692	0.8708	93.71	92.3267	1.3833	13	13.0175	–0.0175
19	85.76	87.4008	–1.6408	81.68	82.53	–0.85	2.45	2.8842	–0.4342
20	92.26	90.4442	1.8158	88.08	86.76	1.32	4.5	4.4242	0.0758
21	80.73	81.7992	–1.0692	76.87	77.48	–0.61	1.5	2.4575	–0.9575
22	85.4	84.1558	1.2442	80.56	79.48	1.08	3.5	2.9008	0.5992
23	86.99	87.3542	–0.3642	82.87	83.9133	–1.0433	4.7	5.5675	–0.8675
24	88.64	88.1008	0.5392	85.29	83.7767	1.5133	4.5	3.9908	0.5092
25	84.83	85.3042	–0.4742	81.12	81.3508	–0.2308	2.5	2.5708	–0.0708
26	86.35	85.3042	1.0458	82	81.3508	0.6492	2.5	2.5708	–0.0708
27	85.16	85.3042	–0.1442	81.56	81.3508	0.2092	2.5	2.5708	–0.0708
28	85.78	85.3042	0.4758	80.15	81.3508	–1.2008	2.45	2.5708	–0.1208
29	86.42	85.3042	1.1158	83.35	81.3508	1.9992	2.5	2.5708	–0.0708
30	84.57	85.3042	–0.7342	82.45	81.3508	1.0992	2.6	2.5708	0.0292
31	86.2	85.3042	0.8958	81.36	81.3508	0.0092	2.5	2.5708	–0.0708
32	84.99	85.3042	–0.3142	80.89	81.3508	–0.4608	3	2.5708	0.4292
33	84.45	85.3042	–0.8542	81.87	81.3508	0.5192	2.7	2.5708	0.1292
34	84.89	85.3042	–0.4142	80.24	81.3508	–1.1108	2.5	2.5708	–0.0708
35	85.01	85.3042	–0.2942	80.98	81.3508	–0.3708	2.5	2.5708	–0.0708
36	85	85.3042	–0.3042	80.24	81.3508	–1.1108	2.6	2.5708	0.0292

that the model accurately predicts the three responses as a function of the four parameters, as seen by the large coefficient of determination R^2 and lower p-value (<0.0001). The determination coefficient R^2 = 0.95 for COD removal, 0.94 for absorbance, and 0.97 for sludge volume are higher with a low p-value (<0.0001); indicating a good correlation between expected and experimental values.

3.5. Optimization process

The purpose of the optimization is to define the right treatment setting for indigo blue dye removal. By using STATISTICAL [54] and JMP [53] software, the response surfaces and the iso-response curves were produced to establish the optimal values of operating parameters for removing indigo blue dye color, COD reduction, and sludge volume.

3.5.1. Optimal domain for high % removal COD response

The three-dimensional response surface plots were developed based on two independent parameters (pH and coagulant dosage) while the other two variables were held constant (concentration dosage and flocculant dosage at

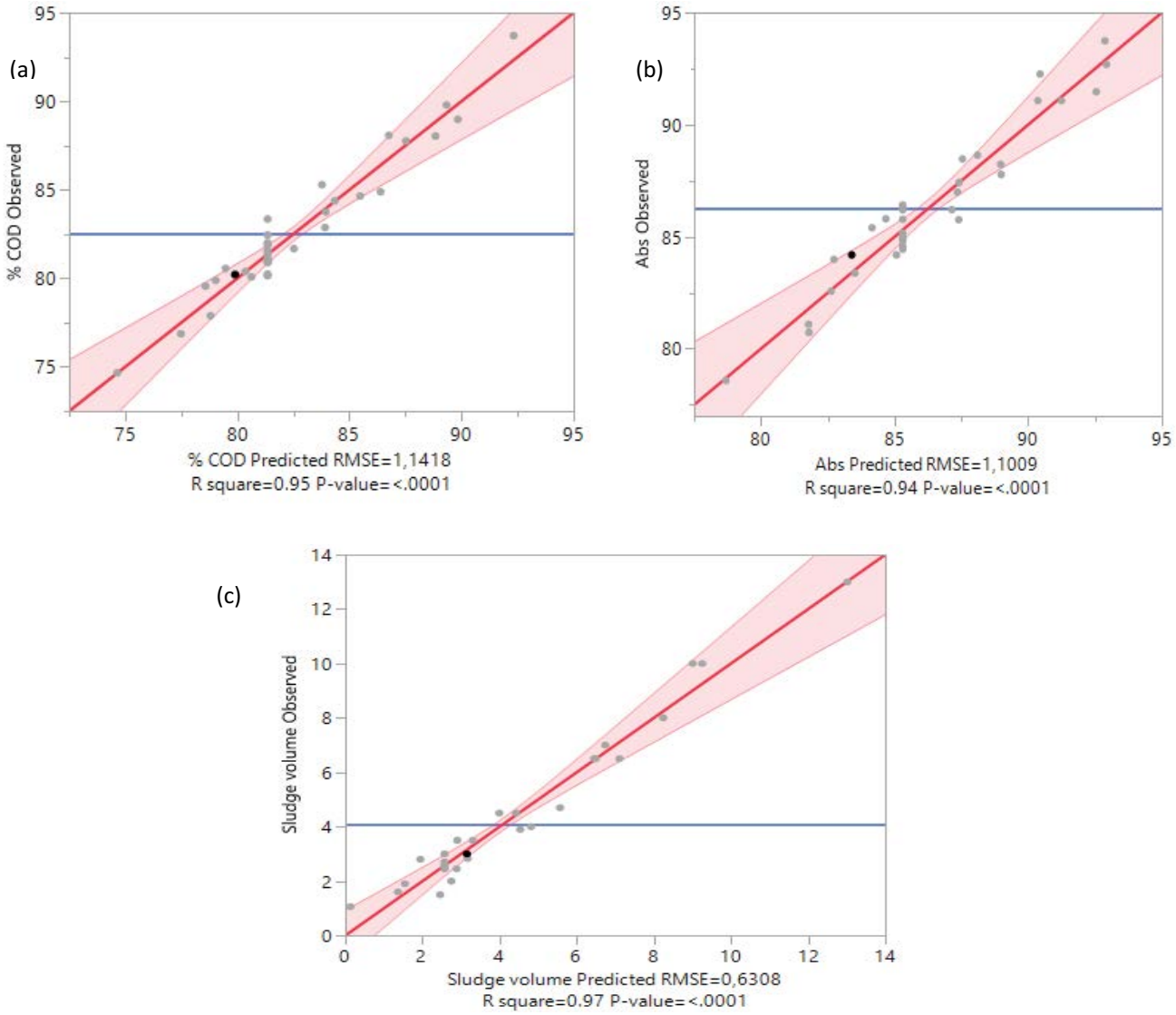

Fig. 8. Graphical representation of the predicted and observed (experimental) values of (a) % of chemical oxygen demand removal, (b) % absorbance (Abs), and (c) volume sludge.

3.23 g/L and 0.94 mL, respectively). According to Fig. 9, the % COD removal rises with increasing pH and coagulant dosage to a minimal level of 80% COD removal and a maximum of 98%. The optimal zone for the highest COD reduction is realized by a pH of around 11.25–11.7 and a coagulant dosage between 4.07–4.25 mL. The effect of pH on COD reduction by an electrocoagulation technique on blue indigo dye has also been observed by Hendaoui et al. [21]. The identification of appropriate locations for the best COD removal is outlined in Table 10.

3.5.2. Optimal domain for % absorbance response

As shown in Fig. 10, the pH increases the effluent decontamination percentage. Fig. 9 indicates that for a fixed value of the same variable (concentration dosage (3.23 g/L) and flocculant dosage (0.94 mL), increasing the pH and coagulant dosage leads to increases in % absorbance with a minimal level of 84% and reaches a maximum 100%. Table 11 summarizes the optimal locations for the good % absorbance.

3.5.3. Optimal domain for sludge volume response

According to Fig. 11, it was observed that when the value of pH and coagulant dosage increase the sludge volume increase also. The same remark has been observed, the sludge volume varies from a minimum value of 1.5 mL corresponding to a pH equal to 7.95 and a coagulant dosage of 2 mL, and a maximum of 15 mL corresponding to pH = 12 and 2.355 mL coagulant dosage. The ideal zone for an optimum sludge volume is in the interval for pH between 11.25 and 11.7 and a coagulant dosage between 4.07 and 4.25 mL while keeping the other two variables constant at 3.23 g/L and 0.94 mL for concentration dose and flocculant dose, respectively. Table 12 provides the appropriate area for optimal sludge volume.

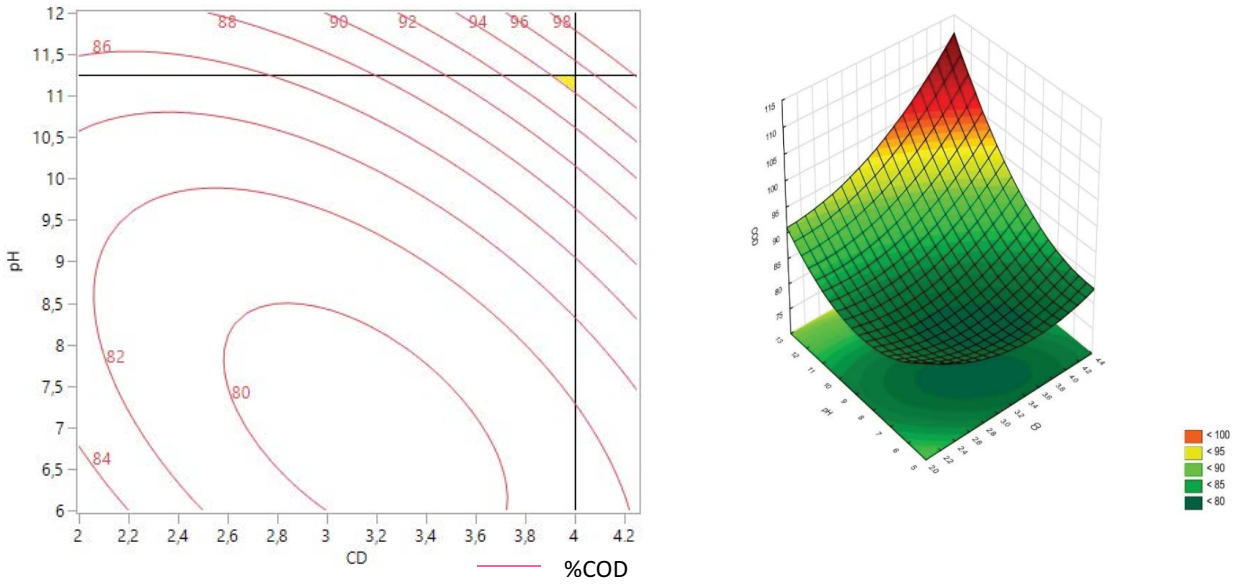

Fig. 9. Response surface and iso-response curves of % chemical oxygen demand removal depending on pH and coagulant dosage; where concentration dose fixed at 3.23 g/L and flocculant dose at 0.94 mL.

Table 10
Optimal domain for chemical oxygen demand response

	Optimal area for chemical oxygen demand removal		% Chemical oxygen demand optimal reduction	
	min.	max.	min.	max.
pH	11.25	11.7	95	98
Coagulant dose (mL)	4.07	4.25		
Concentration dosage (g/L)	3.23			
Flocculant dose (mL)	0.94			

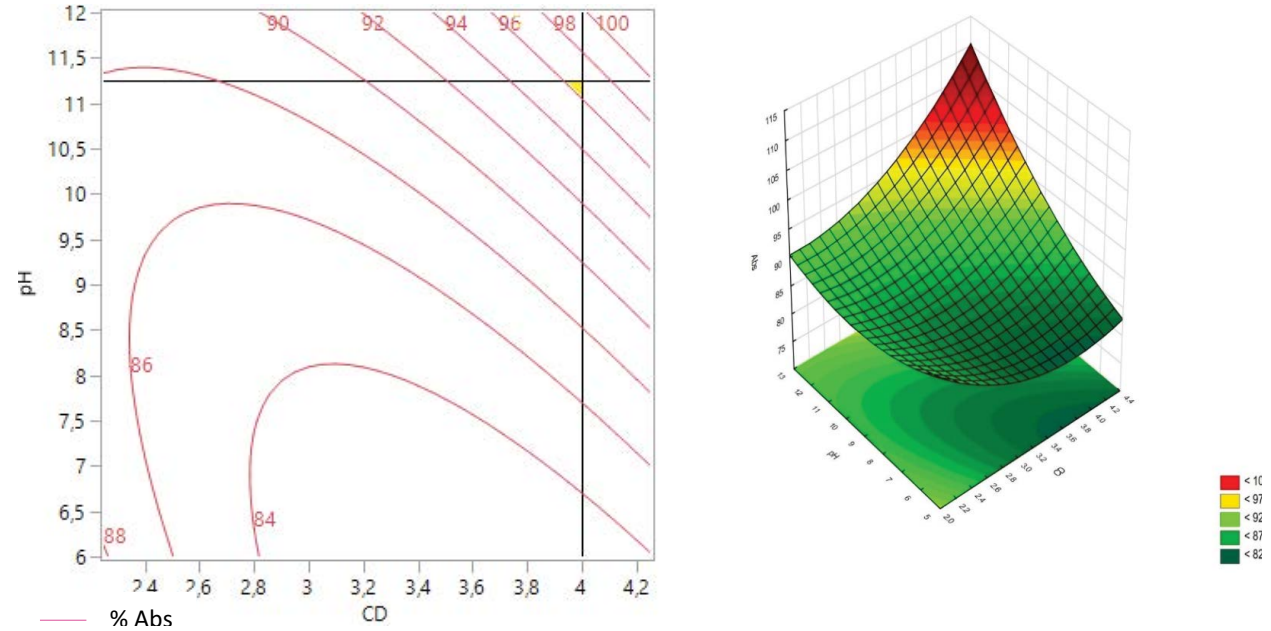

Fig. 10. Response surface and iso-response curves of % absorbance depending on pH and coagulant dosage; where concentration dose fixed at 3.23 g/L and flocculant dose at 0.94 mL.

Table 13 provides the optimal domain for the three responses stated in Tables 10–12, resulting in the highest COD yield, highest absorbance, and lowest sludge volume while accounting for reagent costs, production, and management sludge.

Similarly, the three overlay plots of these three curves 9, 10, and 11 enable us to determine the ideal treatment settings for removing indigo blue dye while keeping an acceptable cost and tacking aspect in the management of sludge volume. Therefore, we can utilize the three contour plots 9, 10 11, and iso-response curves in Fig. 12 to obtain ideal approximate values for these two factors with two variables (coagulant concentration = 3.23 g/L, dose flocculant = 0.94 mL) kept constant around in their central values and the other two others variables (pH and coagulant dose: the elements with the biggest impact) fluctuated within the experimental ranges.

Given the extremely high cost of reagents, we may conclude from these four Figs. 9–12 that a basic pH of around

Table 11
Optimal domain for % absorbance response

	Optimal area for absorbance		% Absorbance optimal reduction	
	min.	max.	min.	max.
pH	11.25	11.7	96	100
Coagulant dose (mL)	4.07	4.25		
Concentration dosage (g/L)	3.23			
Flocculant dose (mL)	0.94			

Table 12
Optimal domain for sludge volume response

	Optimal area for sludge volume		Optimal value of sludge volume (mL)	
	min.	max.	min.	max.
pH	11.25	11.7	10.4	12.3
Coagulant dose (mL)	4.07	4.25		
Concentration dosage (g/L)	3.23			
Flocculant dose (mL)	0.94			

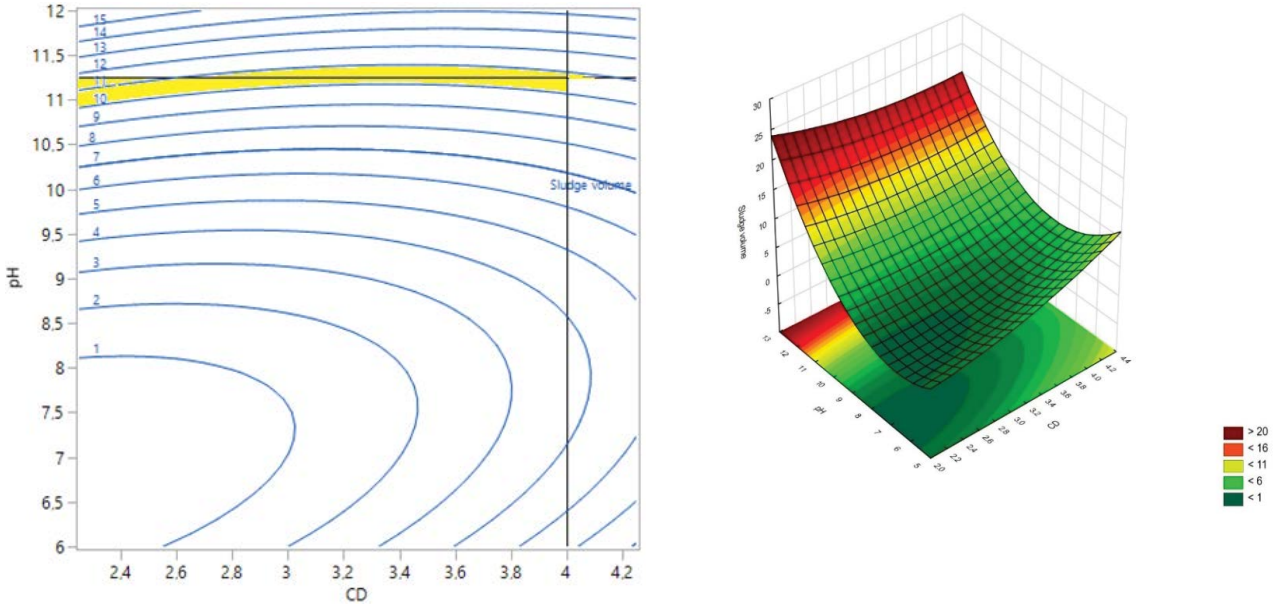

Fig. 11. Response surface and iso-response curves of sludge volume (mL) depending on pH and coagulant dose; where concentration dose fixed at 3.23 g/L and flocculant dose at 0.94 mL.

Table 13
Optimal domain and optimal chemical oxygen demand reduction, maximum absorbance, and sludge volume

Optimal domain of variable			Optimal yield for responses		
	min.	max.		min.	max.
pH	11.25	11.7	% Chemical oxygen demand	95	98
Coagulant dose (mL)	4.07	4.25	% absorbance	96	100
Concentration dose (g/L)	3.23		Sludge volume (mL)	10.4	12.3
Flocculant dose (mL)	0.94				

11.25, a coagulant dose of about 4.07 mL, a concentration of coagulant at 3.23 g/L, and a flocculant dose of about 0.94 mL will result in the highest yield of removal of indigo. Under the ideal operating settings (4.07 mL, 3.23 g/L, 0.94 mL, and 11.25 for coagulant dose, concentration, flocculant dose, and pH, respectively, we can obtain effective COD removal of 96.42%, 98.24% color removal, and 10.40 mL as sludge volume recovery.

Similar findings have been found in the color removal of indigo blue dye by [64–66] with different treatment technologies which reinforces the current conclusion. Furthermore, when compared to other methods (Sono-electrochemical Flow Reactor), it was reasonable to remove up to 90% of the indigo dye [67] and electrocoagulation can reach 93.97% of color removal in the optimal environment [20].

Table 14 shows the optimal treatment settings for treating textile wastewater as well as the predicted COD removal, % absorbance, and sludge volume.

3.6. Experimental validation and characterization of the treated effluent

Three further experiments were run under identical operating settings (Table 14) to ensure that model results can be confirmed by experience. Table 15 demonstrates the close agreement between experimentally obtained COD removal efficiency, absorbance, and sludge volume and model-calculated.

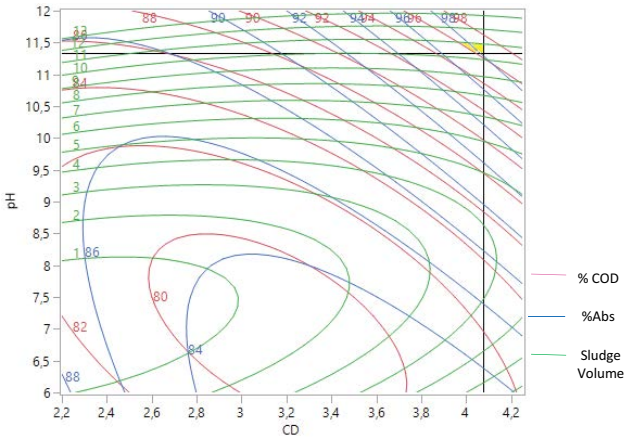

Fig. 12. Iso-response curves for % chemical oxygen demand removal, absorbance (% Abs), and sludge volume under optimal conditions; where concentration dose fixed at 3.23 g/L and flocculant dose at 0.94 mL.

After the experimental validation, an additional characterization of the treated effluent was performed. Table 16 displays the characterization of the treated water under optimal conditions. It can be concluded that all the parameters are conform to the disposal limits except the pH which will be neutralized by the addition of sulfuric acid.

3.7. Comparison between actual and previous studies

The findings of this investigation are better to those others studies (Table 17) tacking consideration the affordability and the efficiency dye removal.

3.8. Density functional theory calculations for indigo blue and $AlCl_3$

The indigo blue and $AlCl_3$ structures were optimized at the B3LYP level of the DFT theory at a 6–31G basis set.

Table 15
Experiments validation at optimal operating conditions

Responses	Experimental value	Model response	Error
Chemical oxygen demand removal (%)	96.28	96.42	–0.14
Absorbance (%)	97.03	98.21	–1.18
Sludge volume (mL)	11	10.40	0.60

Table 16
Characterization of the treated effluent

Physico-chemical characteristics	Value	Disposal limits values (*)
Chemical oxygen demand, mg/L	132.102	900
Absorbance	0.0044	–
Turbidity, NTU	22	–
Conductivity, mS/cm	7.8	–
pH	10.8	5.5–8.5
Temperature, °C	21	30
Total suspended solids (TSS), mg/L	110	400
Color	Clear water	–

Table 14
Optimal operating settings and predicted yield

Parameter	Optimum values	Predicted yield		
		% Chemical oxygen demand removal	% absorbance	Sludge volume (mL)
pH	11.25	96.42	98.21	10.40
Coagulant dose (mL)	4.07			
Concentration coagulant (g/L)	3.23			
Flocculant dose (mL)	0.94			

The quantum chemical values were calculated to elucidate the chemical stability and reactivity behavior of the compound. As known and defined in the 2.3 section, Table 18 provides the electronic properties of indigo blue and $AlCl_3$. As presented in Table 18, indigo blue having E_{HOMO} = −3.5797 eV exhibited a higher charge transfer character when compared to $AlCl_3$ having E_{HOMO} = −9.363 eV. This implies that electron transfer from the indigo blue dye to $AlCl_3$ is simple and will stabilize the system. Other reactivity descriptors which include electrophilicity index (ω) indicated that the coagulant $AlCl_3$ (ω = 6.156 eV, μ = –6.221 eV) acts as an electrophile (electron acceptors) and indigo blue dye as a nucleophilic character (electron donor) (ω = 7.174 eV, μ = –4.168 eV).

The Parr's index calculation P_k^+ and P_k^- of indigo blue dye (Table 19), has shown that the locations with the highest value of ω_k are those that are most susceptible sites to nucleophilic attack on the oxygen bonds (–C_8=O_{10} and C_{11}=O_{19} with ω_k = 1.716 eV). The major proposed interactions between indigo blue dye and $AlCl_3$ are presented in Fig. 13; include Carbon=Oxygen bonding, electrostatic interactions (group O–H), and the radical –Cl (chloride group) which is more electronegative (–0.278 eV). This proposed reaction process

Table 17
Comparison between actual and previous studies

Used dye	Technique/method	Removal efficiency	Time/flow rate	Total cost, USD/m^3	References
Real effluent (indigo)	Coagulation-$AlCl_3$	98.21%	–	0.0826	This study
Blue indigo dye	Fe/Fe-RSM	94.083%	2 L/min	0.0927	[20]
Real effluent (indigo)	Fe/Fe-RSM	95%	11 min	0.92	[68]
Real effluent (indigo)	Al/Al-RSM	96.38%	60 min	–	[66]
Real printing ink	Al/Al	98.7%		0.35–2.71	[69]
Blue indigo dye	Coagulation-alum	97%	–	–	[65]
Pre-treated reel textile effluent	Al/Al	90.3%–94.9%	–	1.5	[70]
Blue indigo dye	Adsorption–ultrafiltration	99%	–	–	[26]
Blue indigo dye	Coagulation-$MgCl_2$	80%	–	–	
Reactive Black 5 dye	EC + Fe^{2+} (1.5 mM Fe^{2+}) process	94.2%	–	1.422	[24]

RSM: response surface methodology.

Table 18
Electronic properties of reagents by DFT at B3LYP/6-31G (the values in eV except E(RB3LYP))

Reagents	E(RB3LYP)*	HOMO	LUMO	ΔE_{gap}	ω	ω^+	ω^-	μ	N
Indigo blue	–875.468	–5.379	–2.957	2.422	7.174	1.806	2.030	–4.168	3.783
$AlCl_3$	–1,623.14	–9.363	3.078	6.286	6.156	0.753	4.715	–6.221	–

(*) the value in atom unit (a.u.).

Table 19
Theoretical prediction of reactive sites using the Parr function for indigo blue (the values in eV)

N° of atom	Atom	P_k^-	P_k^+	ω	N	ω_k	N_k
1	C	0.09668	–0.077662	7.174	3.783	0.69358813	–0.29380703
2	C	–0.053289	0.117067	7.174	3.783	–0.38229849	0.44288207
3	C	0.071185	–0.079629	7.174	3.783	0.51068547	–0.30124849
….	…..	….	…	….	….	….	….
7	**N**	–0.021291	0.260943	7.174	3.783	–0.5274291	**0.98718663**
8	C	0.068976	–0.050686	7.174	3.783	0.49483797	–0.19175276
9	C	0.07367	0.045072	7.174	3.783	0.52851301	0.17051416
10	**O**	0.239227	0.142561	7.174	3.783	**1.71622887**	0.53932971
18	C	0.07367	0.045072	7.174	3.783	0.52851301	0.17051416
19	**O**	0.239227	0.142561	7.174	3.783	**1.71622887**	0.53932971
20	**N**	–0.021291	0.260943	7.174	3.783	–0.15274291	**0.98718663**
….	…..	….	…	….	….	….	….
30	H	–0.003128	0.000877	7.174	3.783	–0.02244046	0.00331782

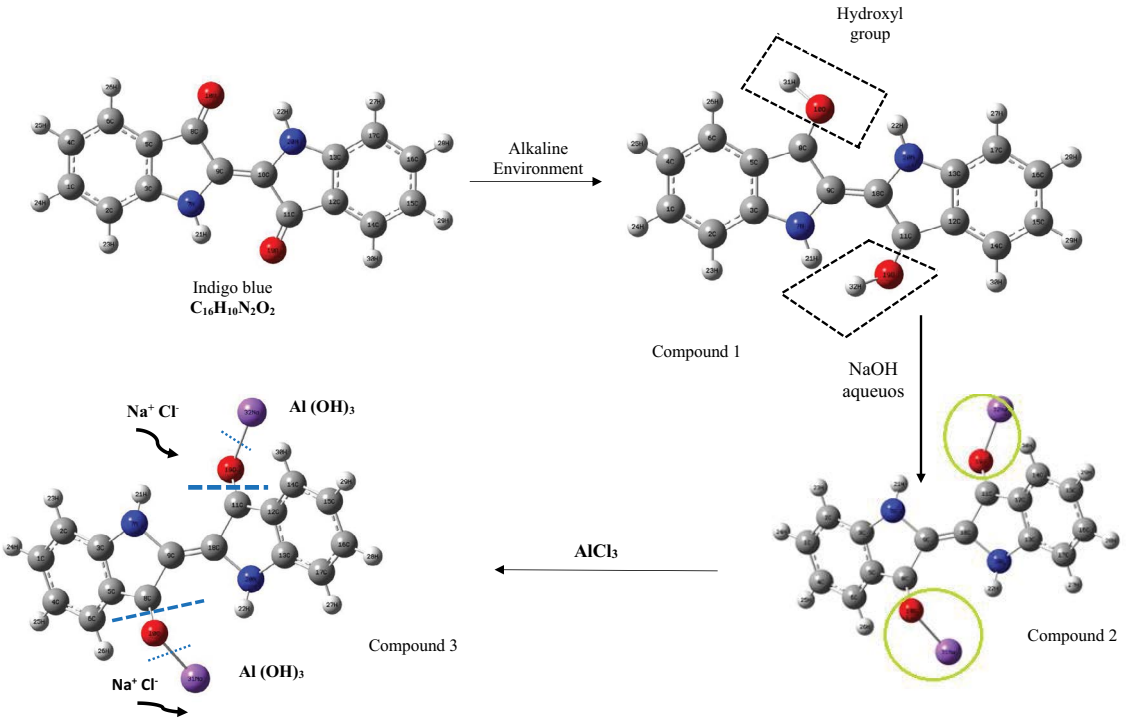

Fig. 13. Reaction mechanism of indigo blue removal by $AlCl_3$ in an alkaline environment.

is comparable to that proposed by [71], in his study on the coagulation of indigo carmine by $FeCl_3$. Under basic conditions (pH = 11.25) with NaOH, the anionic indigo blue dye's negatively charged molecules interact (O groups or –NH– bonds) with the positively charged coagulant functional groups (Al groups). Through analysis of quantum parameter values, oxygen bonds (–C8=O10 and C11=O19 were primarily responsible for the coagulation process. Therefore, this study could be useful in providing critical information for evaluating the removal efficiency and a feasible way to predict the removal rate of dyes by $AlCl_3$ when no coagulation experiments were conducted.

To link the results from the DFT to the experimental study, we can conclude that the hydroxyl group (–OH) is attached to the indigo blue (compound 1), while Na^+ is fixed on the O-group (compound 2). And, with $AlCl_3$, the suspected nucleophilic attack sites in compound 2 lead to –CO loss to form compound 3 (Al^+ was complexed with oxygen while the –Cl group was complexed with Na^+, resulting in a precipitate of NaCl (compound 3)). The density functional theory calculation confirmed the involvement of –C=O, –Cl, and –OH groups in the nucleophilic reaction between indigo blue and $AlCl_3$, and this research could provide a reference value that highlights the importance of introducing the DFT in the domain of industrial wastewater treatment.

Where: $\omega_k = \omega P_k^+$

$N_k = NP_k^-$

Where ω and N are the electrophilicity and nucleophilicity index, respectively (Table 18).

And $P_k^+ = \rho_s^{rc}(r)$ for electrophilic attacks,

$P_k^- = \rho_s^{ra}(r)$ for nucleophilic attacks

where $\rho_s^{rc}(r)$ is the atomic spin density (ASD) of the radical cation, and $\rho_s^{ra}(r)$ is the ASD of the radical anion.

4. Conclusion

The current work allowed us to address the issue of removing indigo blue from industrial wastewaters. A combined experimental (orthogonal central composite design (CCD) and theoretical (density functional theory) approach have been used to further understand the effect of various variables on the treatment of real textile wastewater, containing indigo blue, in a continuous flow reactor using aluminum chloride coagulant ($AlCl_3$) and cationic flocculant (Himoloc DR3000). This allowed to emphasize chemical interactions between the reagent aluminum chloride ($AlCl_3$) and indigo blue dye and we describe the action mode between the effluent and the coagulant by identifying the most vulnerable locations to nucleophilic attacks.

Analysis of the examined parameters' effects on the three responses (COD removal, absorbance, and sludge volume) revealed that all of the variables have a substantial impact on the treatment generally, with the pH having the strongest influence. The response surfaces (3D) and iso-response curves (2D) generated from the regression equations facilitated the identification of the ideal operating settings (4.07 mL, 3.23 g/L, 0.94 mL, and 11.25 for coagulant dose, concentration, flocculant dose, and pH, respectively) leading to achieving maximum efficiency of indigo blue removal (96.42% for COD removal, 98.21% for absorbance, and 10.40 mL for sludge volume) with a total cost of 0.0826 USD/m^3.

Density functional theory (DFT) results in analysis revealed that $AlCl_3$ (ω = 6.156 eV) acts as an electrophile and the indigo blue dye (ω = 7.174 eV) as a nucleophile and demonstrated that the indigo blue molecular structure was particularly vulnerable to nucleophilic attack at the bonding area –C8=O10 and –C11=O19, (with ω_k = 1.716 eV).

The major proposed interactions between indigo blue and $AlCl_3$ include carbon–oxygen bonding and electrostatic interactions (group O–H).

Finally, the developed model may emphasize the process engineering aspects of industrial wastewater treatment, and the linking with theoretical data could explain the involved removal mechanisms.

Data availability

The datasets generated during and/or analyzed during the current study are available from the corresponding author on reasonable request.

Code availability

Not applicable.

Acknowledgements

The authors would like to thank the manager of the sky wash company for their technical assistance, particularly during the collection and delivery of the textile effluent.

Funding

This research did not receive any specific grant from funding agencies in the public, commercial, or not-for-profit sectors.

Author information

Authors and affiliations

Laboratory of Process Engineering and Environment, Faculty of Sciences and Technology Mohammedia, B.P 146 Univ. Hassan II, Casablanca, Morocco.

Slimane EL Harfaoui, Ali Mohssine, Anas Driouich, Khalid Digua, Hassan Chaair.

Laboratory of advanced materials and process engineering, Faculty of Sciences Kenitra, Univ. Ibn Tofail, B.P 242 Kenitra, Morocco.

Zakia Zmirli, Brahim Sallek.

Contributions

Slimane EL Harfaoui: Conceptualization, Data curation, Formal analysis and Investigation, Methodology, Writing – original draft preparation, validation, Visualization.

Zakia Zmirli: Methodology, review, and Editing.

Ali Mohssine: Review and Editing, Formal analysis.

Anas Driouich: Methodology, Software, Formal analysis, Validation, Investigation

Brahim Sallek: Methodology, review, and Editing.

Khalid Digua: Supervision, Investigation, Review, and Editing.

Hassan Chaair: Conceptualization, Supervision, Investigation, Review, and Editing.

Corresponding author

Correspondence to (H. CHAAIR) hassan.chaair@uni-vh2c.ma

Ethics declarations

Ethics approval

Not applicable.

Consent to participate

Not applicable.

Consent for publication

Not applicable.

Competing interests

The authors declare no competing interests.

References

[1] H.B. Mansour, O. Boughzala, dorra Dridi, D. Barillier, L. Chekir-Ghedira, R. Mosrati, Les colorants textiles sources de contamination de l'eau: CRIBLAGE de la toxicité et des méthodes de traitement, Rev. Sci. L'eau, 24 (2011) 209–238.

[2] M. Berradi, R. Hsissou, M. Khudhair, M. Assouag, O. Cherkaoui, A. El Bachiri, A. El Harfi, Textile finishing dyes and their impact on aquatic environs, Heliyon, 5 (2019) e02711, doi: 10.1016/j.heliyon.2019.e02711.

[3] Md. A. Islam, I. Ali, S.M. Abdul Karim, Md. S.H. Firoz, A. Chowdhury, D.W. Morton, M.J. Angove, Removal of dye from polluted water using novel nano manganese oxide-based materials, J. Water Process Eng., 32 (2019) 100911, doi: 10.1016/j.jwpe.2019.100911.

[4] J.N. Etters, Indigo dyeing of cotton denim yarn: correlating theory with practice, J. Soc. Dyers Colour., 109 (1993) 251–255.

[5] K.S. Bharathi, S.T. Ramesh, Removal of dyes using agricultural waste as low-cost adsorbents: a review, Appl. Water Sci., 3 (2013) 773–790.

[6] C.-Q. Zhou, H.-K. Gu, C.-H. Wei, H.-W. Rong, H.Y. Ng, Dyeing and finishing wastewater treatment via a low-cost hybrid process of hydrolysis-acidification and alternately anoxic/oxic sequencing batch reactor with synchronous coagulation, J. Water Process Eng., 49 (2022) 102939, doi: 10.1016/j.jwpe.2022.102939.

[7] V. Katheresan, J. Kansedo, S.Y. Lau, Efficiency of various recent wastewater dye removal methods: a review, J. Environ. Chem. Eng., 6 (2018) 4676–4697.

[8] I. Karapanagiotis, V. de Villemereuil, P. Magiatis, P. Polychronopoulos, K. Vougogiannopoulou, A. Skaltsounis, Identification of the coloring constituents of four natural indigoid dyes, J. Liq. Chromatogr. Relat. Technol., 29 (2006) 1491–1502.

[9] M. de Keijzer, M.R. van Bommel, R.H. Keijzer, R. Knaller, E. Oberhumer, Indigo carmine: understanding a problematic blue dye, Stud. Conserv., 57 (2012) S87–S95.

[10] J. Zhang, Q. Zhou, L. Ou, Removal of indigo carmine from aqueous solution by microwave-treated activated carbon from peanut shell, Desal. Water Treat., 57 (2016) 718–727.

[11] M. Hosseinnezhad, S. Nasiri, M. Fathi, M. Ghahari, K. Gharanjig, Introduction of new configuration of dyes contain indigo group for dye-sensitized solar cells: DFT and photovoltaic study, Opt. Mater., 124 (2022) 111999, doi: 10.1016/j.optmat.2022.111999.

[12] L.F. Albuquerque, A.A. Salgueiro, J.L. de S. Melo, O. Chiavone-Filho, Coagulation of indigo blue present in dyeing wastewater using a residual bittern, Sep. Purif. Technol., 104 (2013) 246–249.

[13] M.F. Chowdhury, S. Khandaker, F. Sarker, A. Islam, M.T. Rahman, Md. R. Awual, Current treatment technologies and mechanisms for removal of Indigo Carmine dyes

from wastewater: a review, J. Mol. Liq., 318 (2020) 114061, doi: 10.1016/j.molliq.2020.114061.
[14] T. Bhagavathi Pushpa, J. Vijayaraghavan, S.J. Sardhar Basha, V. Sekaran, K. Vijayaraghavan, J. Jegan, Investigation on removal of malachite green using EM based compost as adsorbent, Ecotoxicol. Environ. Saf., 118 (2015) 177-182, doi: 10.1016/j.ecoenv.2015.04.033.
[15] T.B. Gupta, D.H. Lataye, Adsorption of Indigo Carmine dye onto *Acacia Nilotica* (Babool) sawdust activated carbon, J. Hazard. Toxic Radioact. Waste, 21 (2017) 04017013, doi: 10.1061/(ASCE) HZ.2153-5515.0000365.
[16] F. Mcyotto, Q. Wei, D.K. Macharia, M. Huang, C. Shen, C.W.K. Chow, Effect of dye structure on color removal efficiency by coagulation, Chem. Eng. J., 405 (2021) 126674, doi: 10.1016/j.cej.2020.126674.
[17] P.R. Yaashikaa, P.S. Kumar, A. Saravanan, D.-V.N. Vo, Advances in biosorbents for removal of environmental pollutants: a review on pretreatment, removal mechanism and future outlook, J. Hazard. Mater., 420 (2021) 126596, doi: 10.1016/j.jhazmat.2021.126596.
[18] B. Shi, G. Li, D. Wang, C. Feng, H. Tang, Removal of direct dyes by coagulation: the performance of preformed polymeric aluminum species, J. Hazard. Mater., 143 (2007), 567–574.
[19] P.W. Wong, T.T. Teng, N.A.R.N. Norulaini, Efficiency of the coagulation–flocculation method for the treatment of dye mixtures containing disperse and reactive dye, Water Qual. Res. J., 42 (2007) 54–62.
[20] K. Hendaoui, M. Trabelsi-Ayadi, F. Ayari, Optimization and mechanisms analysis of indigo dye removal using continuous electrocoagulation, Chin. J. Chem. Eng., 29 (2021) 242–252.
[21] K. Hendaoui, F. Ayari, I.B. Rayana, R.B. Amar, F. Darragi, M. Trabelsi-Ayadi, Real indigo dyeing effluent decontamination using continuous electrocoagulation cell: study and optimization using response surface methodology, Process Saf. Environ. Prot., 116 (2018) 578–589.
[22] Z. Wu, J. Dong, Y. Yao, Y. Yang, F. Wei, Continuous flowing electrocoagulation reactor for efficient removal of azo dyes: kinetic and isotherm studies of adsorption, Environ. Technol. Innovation, 22 (2021) 101448, doi: 10.1016/j.eti.2021.101448.
[23] R. De Maman, V.C. da Luz, L. Behling, A. Dervanoski, C.D. Rosa, G.D.L. Pasquali, Electrocoagulation applied for textile dye oxidation using iron slag as electrodes, Environ. Sci. Pollut. Res., (2021) 1–21, doi: 10.21203/rs.3.rs-477015/v1.
[24] Md. B.K. Suhan, S.B. Shuchi, A. Anis, Z. Haque, Md. S. Islam, Comparative degradation study of Remazol Black B dye using electro-coagulation and electro-Fenton process: kinetics and cost analysis, Environ. Nanotechnol. Monit. Manage., 14 (2020) 100335, doi: 10.1016/j.enmm.2020.100335.
[25] Y.S. Tlaiaa, Z.A.R. Naser, A.H. Ali, Comparison between coagulation and electrocoagulation processes for the removal of Reactive Black dye RB-5 and COD reduction, Desal. Water Treat., 195 (2020) 154–161.
[26] M. Missaoui, N. Tahri, M.O. Daramola, J. Duplay, G. Schäfer, R. Ben Amar, Comparative investigation of indigo blue dye removal efficiency of activated carbon and natural clay in adsorption/ultrafiltration system, Desal. Water Treat., 164 (2019) 326–338.
[27] M. Benjelloun, Y. Miyah, G. Akdemir Evrendilek, F. Zerrouq, S. Lairini, Recent advances in adsorption kinetic models: their application to dye types, Arabian J. Chem., 14 (2021) 103031, doi: 10.1016/j.arabjc.2021.103031.
[28] M. Berradi, A. Essamri, A.E. Harfi, Discoloration of water loaded with vat dyes by the membrane process of ultrafiltration, J. Mater. Environ. Sci., 7 (2016) 1098–1106.
[29] N. Azbar, T. Yonar, K. Kestioglu, Comparison of various advanced oxidation processes and chemical treatment methods for COD and color removal from a polyester and acetate fiber dyeing effluent, Chemosphere, 55 (2004) 35–43.
[30] Q. Zheng, Y. Dai, X. Han, Decolorization of azo dye C.I. Reactive Black 5 by ozonation in aqueous solution: influencing factors, degradation products, reaction pathway and toxicity assessment, Water Sci. Technol., 73 (2016) 1500–1510.
[31] M.M. Sari, Removal of acidic indigo carmine textile dye from aqueous solutions using radiation induced cationic hydrogels, Water Sci. Technol., 61 (2010) 2097–2104.
[32] S. Samsami, M. Mohamadizaniani, M.-H. Sarrafzadeh, E.R. Rene, M. Firoozbahr, Recent advances in the treatment of dye-containing wastewater from textile industries: overview and perspectives, Process Saf. Environ. Prot., 143 (2020) 138–163.
[33] P.D. Saha, P. Bhattacharya, K. Sinha, S. Chowdhury, Biosorption of Congo red and Indigo Carmine by nonviable biomass of a new *Dietzia* strain isolated from the effluent of a textile industry, Desal. Water Treat., 51 (2013) 5840–5847.
[34] H. Eslami T. Zarei Mahmoudabadi, Modified coagulation processes using polyferric chloride and polytitanium tetrachloride for the removal of anionic dye from aqueous solution, Int. J. Environ. Sci. Technol., 19 (2021) 1811–1818.
[35] S. Ghafari, H.A. Aziz, M.H. Isa, A.A. Zinatizadeh, Application of response surface methodology (RSM) to optimize coagulation–flocculation treatment of leachate using poly-aluminum chloride (PAC) and alum, J. Hazard. Mater., 163 (2009) 650–656.
[36] R. Smotraiev, A. Nehrii, E. Koltsova, A. Anohina, K. Sorochkina, H. Ratnaweera, Comparison of wastewater coagulation efficiency of pre-polymerised zirconium and traditional aluminium coagulants, J. Water Process Eng., 47 (2022) 102827, doi: 10.1016/j.jwpe.2022.102827.
[37] V. Golob, A. Vinder, M. Simonic, Efficiency of the coagulation/flocculation method for the treatment of dyebath effluents, Dyes Pigm., 67 (2005) 93–97.
[38] S. Karimifard, M.R. Alavi Moghaddam, Application of response surface methodology in physico-chemical removal of dyes from wastewater: a critical review, Sci. Total Environ., 640–641 (2018) 772–797.
[39] M.A. Bezerra, R.E. Santelli, E.P. Oliveira, L.S. Villar, L.A. Escaleira, Response surface methodology (RSM) as a tool for optimization in analytical chemistry, Talanta, 76 (2008) 965–977.
[40] T. Ntambwe Kambuyi, F. Eddaqaq, A. Driouich, B. Bejjany, B. Lekhlif, H. Mellouk, K. Digua A. Dani, Using response surface methodology (RSM) for optimizing turbidity removal by electrocoagulation/electro-flotation in an internal loop airlift reactor, Water Supply, 19 (2019) 2476–2484.
[41] B.C.Y. Lee, M.S. Mahtab, T.H. Neo, I.H. Farooqi, A. Khursheed, A comprehensive review of design of experiment (DOE) for water and wastewater treatment application – key concepts, methodology and contextualized application, J. Water Process Eng., 47 (2022) 102673, doi: 10.1016/j.jwpe.2022.102673.
[42] S.E. Harfaoui, A. Driouich, A. Mohssine, S. Belouafa, Z. Zmirli, H. Mountacer, K. Digua, H. Chaair, Modelization and optimization of the treatment of the Reactive Black 5 dye from industry effluents using experimental design methodology, Sci. Afr., 16 (2022) e01229, doi: 10.1016/j.sciaf.2022.e01229.
[43] Z. Zmirli, A. Driouich, S.E. Harfaoui, A. Mohssine, H. Mountacer, S. Brahim, H. Chaair, Assessment of the principal factors influencing the silver cyanidation process by using Plackett–Burman experimental design, Sci. Afr., 16 (2022) e01137, doi: 10.1016/j.sciaf.2022.e01137.
[44] APHA, APHA, Standard Methods for the Examination of Water and Wastewater, American Public Health Association, Washington, D.C., 1992.
[45] Ministère délégué auprès du Ministre de l'Energie, des Mines, de l'Eau et de l'Environnement, et chargé de l'Eau (MDCEau), Recueil des textes juridiques relatifs aux ressources en eau au Maroc, 2015, p. 423.
[46] F. Byoud, A. Wakrim, C. Benhsinat, Z. Zaroual, S. El Ghachtouli, A. Tazi, H. Chaair, A. Assabbane, M. Azzi, Electrocoagulation treatment of the food dye waste industry: theoretical and experimental study, J. Mater. Environ. Sci., 8 (2017) 4301–4312.
[47] S. Asad, M.A. Amoozegar, A.A. Pourbabaee, M.N. Sarbolouki, S.M.M. Dastgheib, Decolorization of textile azo dyes by newly isolated halophilic and halotolerant bacteria, Bioresour. Technol., 98 (2007) 2082–2088.
[48] S. Abbasi, M. Mirghorayshi, S. Zinadini, A.A. Zinatizadeh, A novel single continuous electrocoagulation process for

treatment of licorice processing wastewater: optimization of operating factors using RSM, Process Saf. Environ. Prot., 134 (2020) 323–332.
[49] H. Chaair, A. Driouich, S.E.A. El Hassani, F. Chajri, O. Britel, K. Digua, Synthesis and characterization of silicate gel by using sol–gel process: experiments and DFT calculations, Mediterr. J. Chem., 9 (2020) 411–421.
[50] Y. Zhao, D.G. Truhlar, Hybrid meta density functional theory methods for thermochemistry, thermochemical kinetics, and noncovalent interactions: the MPW1B95 and MPWB1K models and comparative assessments for hydrogen bonding and van der Waals interactions, J. Phys. Chem. A, 108 (2004) 6908–6918.
[51] L.R. Domingo, J.A. Sáez, Understanding the mechanism of polar Diels–Alder reactions, Org. Biomol. Chem., 7 (2009) 3576, doi: 10.1039/b909611f.
[52] J.L. Gázquez, A. Cedillo, A. Vela, Electrodonating and electroaccepting powers, J. Phys. Chem. A, 111 (2007), doi: 10.1021/jp065459f.
[53] JMP, SAS Institute Inc., JMP 10 Basic Analysis and Graphing, 2nd ed., USA, 2012.
[54] Statistica, C. WeißStatSoft, Inc., Tulsa, OK.: STATISTICA, Version 8, AStA Adv. Statis. Anal. 91, 2007, pp. 339–341
[55] A.R. Anuf, K. Ramaraj, V.S. Sivasankarapillai, R. Dhanusuraman, J.P. Maran, G. Rajeshkumar, A. Rahdar, A.M. Díez-Pascual, Optimization of electrocoagulation process for treatment of rice mill effluent using response surface methodology, J. Water Process Eng., 49 (2022) 103074, doi: 10.1016/j.jwpe.2022.103074.
[56] A. Driouich, S.E.A. El Hassani, H. Labjar, S. Kassbi, T. Ntambwe Kambuyi, O. Britel, B. Sallek, K. Digua, R. Chroqui, H. Chaair, Modeling and optimizing synthesis of irreversible gel by sol-gel using experimental design, Phosphorus, Sulfur Silicon Relat. Elem., 195 (2020) 50–59.
[57] A. Driouich, F. Chajri, S.E.A. El Hassani, O. Britel, S. Belouafa A. Khabbazi, H. Chaair, Optimization synthesis geopolymer based mixture metakaolin and fly ash activated by alkaline solution, J. Non-Cryst. Solids, 544 (2020) 120197, doi: 10.1016/j.jnoncrysol.2020.120197.
[58] S.E.A. El Hassani, A. Driouich, H. Mellouk, B. Bejjany, A. Dani, H. Chaair, K. Digua, Optimization of Parameters Extraction of Natural Antioxidant from Moroccan Grape Pomace, in Advanced Intelligent Systems for Sustainable Development (AI2SD'2019), Vol. 1104, M. Ezziyyani, Ed., Springer International Publishing, Cham, 2020, pp. 501–513.
[59] S.E.A. El Hassani, A. Driouich, H. Chaair, H. Mellouk, K. Digua, Optimization of activated carbon by chemical activation from grape seeds using the response surface methodology, Desal. Water Treat., 245 (2022) 144–157.
[60] K. Berkalou, A. Nounah, H. Chaair, M. Khamar, R. Boussen, A. Driouich, Modelling and optimizing the solvent extraction of cadmium from phosphoric acid using experimental design, Asian J. Chem., 33 (2021) 637–643.
[61] Fisher, K.H. Esbensen, D. Guyot, F. Westad, L.P. Houmoller, Multivariate Data Analysis – In Practice, An Introduction to Multivariate Data Analysis and Experimental Design, Aalborg University, Esbjerg, Denmark, 2002.
[62] H. Eslami, M.H. Ehrampoush, A. Esmaeili, M.H. Salmani, A.A. Ebrahimi, M.T. Ghaneian, H. Falahzadeh, R.F. Fard, Enhanced coagulation process by Fe–Mn bimetal nano-oxides in combination with inorganic polymer coagulants for improving As(V) removal from contaminated water, J. Cleaner Prod., 208 (2019) 384–392.
[63] M.R. Islam, M.G. Mostafa, Characterization of textile dyeing effluent and its treatment using polyaluminum chloride, Appl. Water Sci., 10 (2020) 119, doi: 10.1007/s13201-020-01204-4.
[64] Ö. Gökkuş, Y.Ş. Yıldız, B. Yavuz, Optimization of chemical coagulation of real textile wastewater using Taguchi experimental design method, Desal. Water Treat., 49 (2012) 263–271.
[65] B. Manu, Physico-chemical treatment of indigo dye wastewater, Color. Technol., 123 (2007) 197–202.
[66] S. Prayochmee, P. Weerayutsil, K. Khuanmar, Response surface optimization of electrocoagulation to treat real indigo dye wastewater, Pol. J. Environ. Stud., 30 (2021) 2265–2271.
[67] A. Trujillo-Ortega, S.A.M. Delgadillo, V.X. Mendoza-Escamilla, M. May-Lozano, C. Barrera-Díaz, Modeling the removal of indigo dye from aqueous media in a sonoelectrochemical flow reactor, Int. J. Electrochem. Sci., 8 (2013) 3876–3887.
[68] E. GilPavas, S. Correa-Sanchez, Assessment of the optimized treatment of indigo-polluted industrial textile wastewater by a sequential electrocoagulation-activated carbon adsorption process, J. Water Process Eng., 36 (2020) 101306, doi: 10.1016/j.jwpe.2020.101306.
[69] K.P. Papadopoulos, R. Argyriou, C.N. Economou, N. Charalampous, S. Dailianis, T.I. Tatoulis, A.G. Tekerlekopoulou, D.V. Vayenas, Treatment of printing ink wastewater using electrocoagulation, J. Environ. Manage., 237 (2019) 442–448.
[70] S. Bener, Ö. Bulca, B. Palas, G. Tekin, S. Atalay, G. Ersöz, Electrocoagulation process for the treatment of real textile wastewater: effect of operative conditions on the organic carbon removal and kinetic study, Process Saf. Environ. Prot., 129 (2019) 47–54.
[71] Y. Ren, Y. Tan, Z. Cheng, Y. Liu, S. Liu, Z. Shen, M. Fan, QSAR model and mechanism research on color removal efficiency of dying wastewater by $FeCl_3$ coagulation, Ecotoxicol. Environ. Saf., 240 (2022) 113693, doi: 10.1016/j.ecoenv.2022.113693.